Energy 67 (2014) 575–583

Contents lists available at ScienceDirect

Energy

journal homepage: www.elsevier.com/locate/energy

Electrochemical performance study of solid oxide fuel cell using lattice Boltzmann method

Han Xu [a,b], Zheng Dang [b,*], Bo-Feng Bai [a]

[a] State Key Laboratory of Multiphase Flow in Power Engineering, Xi'an Jiaotong University, Xi'an 710049, China
[b] Dept. of Building Environment and Energy Engineering, Xi'an Jiaotong University, Xi'an 710049, China

ARTICLE INFO

Article history:
Received 22 September 2013
Received in revised form
22 January 2014
Accepted 4 February 2014
Available online 28 February 2014

Keywords:
Solid oxide fuel cell
Lattice Boltzmann method
Electrochemical model
Overpotentials
Mass transfer

ABSTRACT

A comprehensive numerical model was developed to predict the electrochemical performance of solid oxide fuel cell (SOFC). The multi-component Lattice Boltzmann (LB) model based on kinetic theory for gas mixtures combined with a representative elementary volume (REV) scale LB algorithm based on the Brinkman equation for flows in porous media, the Butler–Volmer equation and Ohm's law were adopted to deal with the concentration, activation and ohmic overpotentials, respectively. The volt–ampere characteristics were calculated and compared with those obtained by the existing electrochemical model, as well as the experimental data. It was shown that the electrochemical model given by this paper was capable of describing the electrochemical performance much more accurately because of the kinetic nature of the LB method which was based on microscopic models and mesoscopic kinetic equations for fluids, and the accurate prediction of multi-component mass transfer in SOFC porous electrodes affected the simulation of the cell electrochemical performance significantly. Moreover, the effects of different electrode geometrical and operating parameters on the cell performance were investigated. The developed electrochemical model based on LB algorithm at REV scale is useful for the design and optimization of SOFC.

1. Introduction

Solid oxide fuel cell (SOFC), with advantages of high electric efficiency, low pollutant emission, and high operating temperature which allows a variety of cogeneration possibilities and fuel flexibility, is identified as one of the most promising energy conversion devices in future. However, several pressing technological barriers related to energy conversion efficiency, fuel reforming techniques, the use of novel materials, architecture design, and techniques for improved fuel utilization, etc., which may result in high production costs and reduced reliability of SOFC [1,2], still exist to its commercialization. Because the problems concerning single cells have not been totally eradicated, the design and optimization of SOFC stack and relevant thermodynamic systems are caught in a dilemma [3]. The electrochemical characteristics of the single cell are very important for the SOFC design, which directly affect the cell power generation performance, temperature management, etc. and are influenced significantly by the three polarizations (activation, ohmic and concentration polarization) within electrolyte and electrodes. Statistics show that the vast majority of the published articles about SOFC are devoted to the research about anode, cathode and electrolyte [3].

Numerical simulation is thought to be an important approach to the research of SOFC. The accuracy of overpotential models directly affects the precise simulation of the SOFC electrochemical performance. Generally speaking, Butler–Volmer equation (or Achenbach model) and Ohm's law are usually used to determine the activation and ohmic overpotentials, respectively. However, the research about concentration overpotential is relatively rare, and it is unspecified and not fully resolved in the literature concerning to what degree the mass transfer affects the electrochemical performance of the SOFC [3]. There are three frequently used modeling approaches: (1) concentration overpotential is usually ignored because the gas transport in the electrode is believed to be an efficient process [4–6]; (2) the mass transfer in the porous electrodes is not calculated, and the concentration overpotential is predicted using limiting current density which is usually assumed to be an estimated constant [7,8] or a function with respect to gas concentration, pressure at the gas channel of fuel cell, effective diffusion coefficient, temperature and geometrical structure of

* Corresponding author.
E-mail address: zdang@mail.xjtu.edu.cn (Z. Dang).

http://dx.doi.org/10.1016/j.energy.2014.02.021
0360-5442/

electrodes [9–12]; (3) the mass transfer in the porous electrodes is described by simplified macroscopic models [2,13,14] (extended Fick's model (extended FM), Dusty Gas model (DGM), and Stefan Maxwell model (SMM)), and the concentration overpotential is expressed in terms of the gas concentration difference between the electrodes surface and three phase boundary (TPB) regions. It is clear from our previous research that the concentration overpotential reaches the same order of magnitude as the other two overpotentials for low porosity, low reactant concentrations, and high average current densities [15]. Therefore, the neglect of concentration loss is unreasonable for the fact that the reactant concentration and current density vary sharply along the flow channel of fuel cell, and they achieve the minimum and the maximum at where the electrochemical reaction occurs dramatically, respectively. Meanwhile, the employed limiting current density and aforementioned simplified macroscopic models (extended FM, DGM, and SMM) for concentration overpotential may result in imprecise prediction of the polarization loss of fuel cell because they are not competent to study the gas transport accurately in the porous electrodes at micro- or meso-scale.

The Lattice Boltzmann (LB) method is thought to be an efficient tool for the simulation of multi-component mass transfer in porous anode and cathode. It is deduced from the kinetic theory which makes it capable of solving transport process at micro- or meso-scale. Meanwhile, this algorithm is parallel in nature due to the fact that all the information transfer is local in time and space, so that it is relatively easier to implement and more suitable for the massively parallel computation. Based upon the above mentioned advantages of LB method, several references employed pore scale LB method for the investigation of multi-component gas transport in SOFC porous anode [16–23]. Compared with the pore scale LB model in which detailed geometric information is needed and the computation domain cannot be too large due to limited computer resources, representative elementary volume (REV) scale LB model can be used for systems of larger size and is much more competitive for parametric study. In the researches using REV scale LB method for the multi-component gas transport in porous media [24–29], the majority have adopted single-fluid model employing single-relaxation-time approximation which is restricted to unity Prandtl and Schmidt numbers for the multi-species flow [24–28] or taken the species concentration field as a passive scalar [29]. Nevertheless, the relatively more accurate two-fluid model, which treats mutual collisions and self-collisions independently so that the viscosity and diffusion coefficients can be varied independently by a proper choice of mutual- and self-collision relaxation-time scales, has not been adopted. Furthermore, the REV scale LB model has rarely been applied to the simulation of mass transfer of SOFC electrodes [15].

In our previous research, a two-dimensional (2D) multi-species LB model based on the two-fluid theory coupled with a porous model at REV scale was developed to study the multi-component reactant gases transport in the porous anode and cathode of SOFC, and the prediction of concentration overpotential agree much better with the experimental data compared with those obtained by extended FM, DGM, and SMM, which proves that LB method is a much more accurate method for the simulation of mass transfer within fuel cell electrodes [15]. This paper presents a subsequent investigation of our previous work, in which a comprehensive electrochemical model is established based on the existing LB model developed by our group in Ref. [15] to study the electrochemical characteristics of a planar anode-supported SOFC. The influence of multi-component reactant gas mass transfer on the electrochemical performance of SOFC is investigated. Furthermore, the established model is also applied to discuss the impacts of geometrical and operating parameters on the cell electrochemical performance, which is very useful for the design, optimization and fabrication of SOFC.

2. Mathematical models

Fig. 1 illustrates the schematic of the representative element volume of a planar SOFC which consists of a dense ceramic electrolyte sandwiched between porous anode and cathode. At the cathode, oxygen from the air channel diffuses to the TPB, and receives electrons to be reduced to oxygen ions which pass through the solid oxide electrolyte to the anode. At the anode, hydrogen from the fuel channel diffuses to the TPB, and reacts with the oxygen ions to generate steam and electrons. Finally, the electrons formed in the hydrogen oxidation reaction migrate to the cathode by external circuit to meet the electrical load.

2.1. Conservation equations

Conservation equations for multi-species gas in porous anode and cathode are given as follows.

Continuity equation:

$$\nabla \cdot \vec{u} = 0 \tag{1}$$

Momentum equation:

$$\nabla p = -\frac{\mu}{K}\vec{u} + \mu_e \nabla^2 \vec{u} \tag{2}$$

Species equations:

$$\nabla \cdot J_A = 0 \tag{3}$$

where A represents H_2 or H_2O in the anode, and O_2 or N_2 in the cathode.

In the LB method, Eqs. (1)–(3) are satisfied with calculations of distribution functions by solving the LB equation, which has been introduced in detail in Section 3.

2.2. Electrochemical model

Fig. 2 shows the equivalent circuit model for the calculation of SOFC electrochemical characteristics, from which we have obtained some important equations as summarized in Table 1.

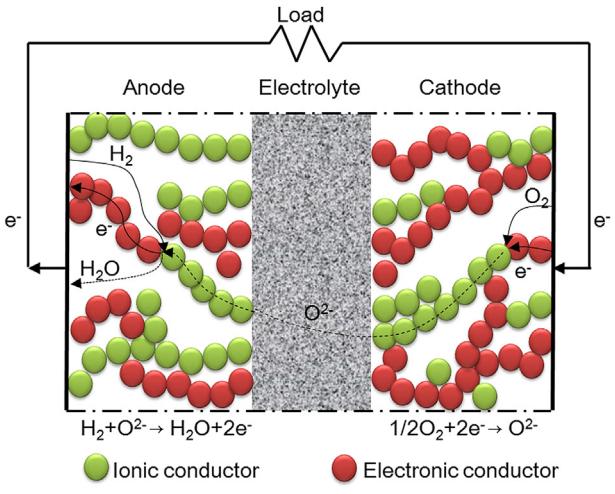

Fig. 1. Schematic of an SOFC representative element volume.

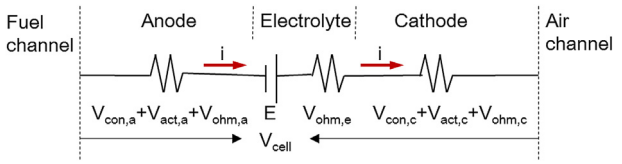

Fig. 2. Equivalent circuit of SOFC electrochemical model.

3. Lattice Boltzmann method

The LB method adopts particle distribution function $f_\alpha^\sigma(\vec{x},t)$ as the primary variable which can be defined for every species 'σ' moving in direction α with a velocity vector of $\vec{e}_\alpha^\sigma$ at each lattice point $\vec{x}$ and time t. The $f_\alpha^\sigma(\vec{x},t)$ is solved by imposing streaming and collision steps over a numerical grid that consists of discrete and regularly spaced lattice points (the D2Q9 model with nine velocity directions on the 2D square lattice for the 2D simulation has been adopted in this study). The macroscopic quantities that describe the fluid flow can be calculated as moments of $f_\alpha^\sigma(\vec{x},t)$.

The coupled LB model for multi-species gas transport in porous media is composed of the LB model for multi-component flow and the LB model for porous flow. As for the LB model that describes porous flow at REV scale, the single-fluid model which is inferior to the two-fluid model is applied for the multi-component flow in the existing publications. Furthermore, it is rarely applied to SOFC. In this paper, a LB model which is based on the two-fluid model initially proposed by Luo and Girimaji [31] derived from the kinetic model for gas mixtures given by Sirovich [32], and extended by McCracken and Abraham [33] in order to model components with different molecular weights is employed for the multi-component flow. As for porous flow, the interaction force of fluid and solid skeleton is included by Guo-Zheng-Shi (GZS) model [34] in which the discrete lattice effect and the contribution of the force term $F_\alpha^\sigma\delta t$ to the momentum flux are both taken into consideration. The binary mixture is taken as an example to describe the coupled LB model. The discrete equation of the species σ is expressed as follows:

$$f_\alpha^\sigma(\vec{x}+\vec{e}_\alpha^\sigma\delta t, t+\delta t) - f_\alpha^\sigma(\vec{x},t) = J_\alpha^{\sigma\sigma} + J_\alpha^{\sigma s} + F_\alpha^\sigma\delta t \tag{13}$$

The velocity set $\vec{e}_\alpha^1$ for species 1 (having the least molecular weight) is given according to the D2Q9 model. For the remaining species, the discrete velocities are obtained by the different lattice speed (DLS) scheme [33]. Streaming of species with different discrete velocities is carried out via bi-linear interpolation [16].

$J_\alpha^{\sigma\sigma}$ is the self-collision term which is approximated by the Bhatnagar–Gross–Krook (BGK) model. $J_\alpha^{\sigma s}$ is the cross-collision term which represents the effect of collisions between particles of various species and arises only when there is more than one species and the relative velocity between particles of different species is non-zero. $F_\alpha^\sigma\delta t$ is the force term to describe the interaction force of fluid and solid skeleton.

$$J_\alpha^{\sigma\sigma} = -\frac{1}{\tau^\sigma}\left[f_\alpha^\sigma - f_\alpha^{\sigma(0)}\right] \tag{14}$$

$$J_\alpha^{\sigma s} = -\frac{1}{\tau_D^{\sigma s}}\frac{\rho_s}{\rho}\frac{f_\alpha^{\sigma(\mathrm{eq})}}{c_{s,\sigma}^2}\left(\vec{e}_\alpha^\sigma - \vec{u}\right)\left(\vec{u}_\sigma - \vec{u}_s\right) \tag{15}$$

$$F_\alpha^\sigma = w_\alpha\rho_\sigma\left(1-\frac{1}{2\tau_\sigma}\right)\left[\frac{\vec{e}_\alpha^\sigma\cdot\vec{a}_\sigma}{c_{s,\sigma}^2} + \frac{\left(\vec{e}_\alpha^\sigma\cdot\vec{u}\right)\left(\vec{e}_\alpha^\sigma\cdot\vec{a}_\sigma\right)}{c_{s,\sigma}^4} - \frac{\vec{u}\cdot\vec{a}_\sigma}{c_{s,\sigma}^2}\right] \tag{16}$$

where ρ_σ and ρ_s, $\vec{u}_\sigma$ and $\vec{\mu}_s$ are the mass densities and flow velocities for species σ and s, and they are moments of distribution functions:

$$\rho_\sigma = \sum_\alpha f_\alpha^\sigma \tag{17}$$

$$\rho_\sigma\vec{u}_\sigma = \sum_\alpha f_\alpha^\sigma\vec{e}_\alpha^\sigma + \frac{\delta t}{2}\rho_\sigma\vec{a}_\sigma \tag{18}$$

where $\vec{a}_\alpha = -\nu/K\vec{u}$ represents the body force due to the presence of a porous media which is needed to recover the Brinkman equation.

$f_\alpha^{\sigma(0)}$ is the equilibrium distribution function, ρ and $\vec{u}$ are the mass density and the velocity of the mixture, τ^σ is the relaxation time of the self-collision term controlling the kinematic viscosity, and $\tau_D^{\sigma s}$ is the relaxation time of the cross-collision term determining the inter-species diffusivities. Much more model descriptions and boundary condition implementation were introduced in Ref. [15] in more details.

4. Results and discussion

4.1. Model validation

The LB model for the multi-component gas transport has been validated with the extended FM, SMM and DGM, as well as the experimental data published by Yakabe et al. at 3000, 7000 and 10,000 A m^{-2} in our previous study [15], and it is proved that the present LB model is capable of simulating the multi-component mass transfer much more accurately in the porous electrodes of SOFC under a wider range of operating conditions. Then the validated LB model, coupled with Butler–Volmer equation and Ohm's law, is employed to simulate the concentration, activation, and ohmic overpotentials. The SOFC volt–ampere characteristics are used for the electrochemical model validation, and Table 2 describes relevant input parameters. Comparisons of the results obtained by the present electrochemical model with those given by Ni et al. [35] as well as experimental data measured by Zhao and Virkar [36] are shown in Fig. 3. We can find that the calculation result using the present model is almost overlapped with the measured value when the current density is below about 15,000 A m^{-2} which includes the vast majority of the SOFC operation conditions. As the current density increases further above 15,000 A m^{-2}, it is also closer to the experimental data in contrast with that of Ni et al. [35].

The electrochemical model adopted by Ni et al. [35] and that in this paper employ the same ohmic overpotential model, but different activation and concentration overpotential models. As for the activation model, both of them use Butler–Volmer equation, but with different expressions of exchange current density. Ni et al. [35] introduce exchange current density depending on gas concentration, operating pressure and temperature, and it is treated as a fitting exponential function of temperature in this paper. However, both of the two expressions have the same anode and cathode exchange current densities at 1073 K (about 5300 A m^{-2} for anode and 2000 A m^{-2} for cathode [30,35]). Therefore, the better prediction of the volt–ampere characteristics in this paper primarily results from the much more precise simulation of the concentration overpotential. The LB method and the extended FM are employed

Table 1
Summary of equations and parameters employed in the SOFC electrochemical model.

Output voltage	$V_{cell} = E - V_{con,a} - V_{act,a} - V_{ohm} - V_{con,c} - V_{act,c}$	(4)
Electromotive force	$E = -\Delta g/2F$	(5)
	where	
	$-\Delta g = -\Delta g^0 + RT\ln\left[\frac{p_{H_2}/p_0(p_{O_2}/p_0)^{1/2}}{p_{H_2O}/p_0}\right]$	(6)
Activation overpotential [14]	$V_{act} = \frac{RT}{F}\sinh^{-1}\left(\frac{i}{2i_o}\right)$	(7)
	where the 'apparent' exchange current density i_o is treated as an exponential function of temperature [30]	
Ohmic overpotential	$V_{ohm} = \sum jr_k \quad (k = \text{anode, electrolyte, cathode})$	(8)
Concentration overpotential	$V_{con,a} = -\frac{RT}{2F}\ln\left(\frac{y_{H_2,A/E}y_{H_2O,bulk}}{y_{H_2,bulk}y_{H_2O,A/E}}\right)$	(9)
	$V_{con,c} = -\frac{RT}{2F}\ln\left(\frac{y_{O_2,A/E}}{y_{O_2,bulk}}\right)^{1/2}$	(10)
	where the molar fraction distribution of each component is simulated by LB method	
Cell power density	$P = iV_{cell}$	(11)
Electrochemical efficiency	$\eta = V_{cell}/E$	(12)

to describe the multi-component gas transport in porous electrodes in this paper and Ref. [35], respectively. It has been proved in our previous study [15] that the concentration overpotential described by extended FM agrees the worst with the experimental results compared with that given by SMM, DGM and LB method. The extended FM has been proved to overestimate the concentration overpotential, and the overestimation becomes increasingly greater as current density rises, which is the reason that the cell voltage predicted by Ni et al. [35] is lower than the experimental result and the dissimilarity tends to be even more remarkable with the increase of the current density. It is also suggested in our previous study [15] that the concentration overpotential obtained by LB model is almost the same as the experimental data in low current density regions, and its underestimation will occur as the current density is above 10,000 A m^{-2}. That's why the cell voltage predicted

Table 2
Input parameters used in model validation and standard case.

Parameter	Value
Operating pressure/bar	1
Fuel composition/air composition	97%H_2, 3%H_2O/21%O_2, 79%N_2
For model validation	
Operating temperature/K	1073
Anode thickness/m	1000×10^{-6}
Cathode thickness/m	20×10^{-6}
Electrolyte thickness/m	8×10^{-6}
Porosity	0.48
Tortuosity	5.4
Standard case	
Operating temperature/K	1023
Average current density/A m^{-2}	10,000
Anode thickness/m	750×10^{-6}
Cathode thickness/m	50×10^{-6}
Electrolyte thickness/m	50×10^{-6}
Porosity	0.46
Tortuosity	4.5
Average pore diameter/m	2.6×10^{-6}
Permeability	1.7×10^{-10}

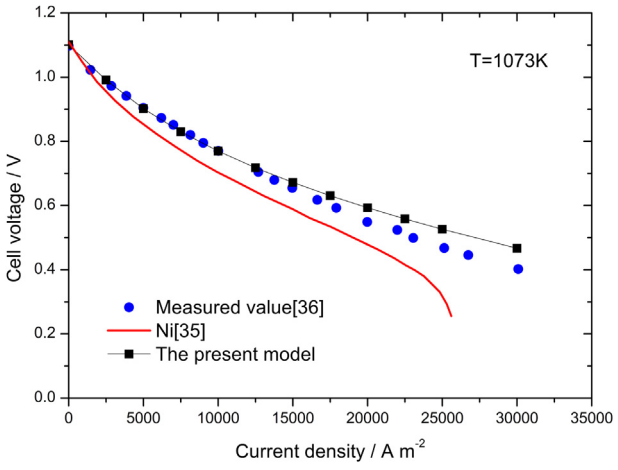

Fig. 3. Comparison of volt–ampere characteristics calculated by the present model with experimental data [36] and predictions given by Ni et al. [35].

by LB model is much closer to the measured value compared with the results given by Ni et al. [35], especially at low current densities, and is increasingly higher than the measured value as the current density increases.

There are three possible reasons making the present simulation method a more robust model. Firstly, the LB model for the multi-component mass transfer in porous electrodes adopted in this paper takes into account both diffusion and convection transport; nevertheless, extended FM in Ref. [35] neglects the convection transport. Secondly, some geometrical parameters (e.g. average pore size) obtained by experiments with several inevitable test errors are needed in the extended FM; however, the LB model is independent of these parameters. The less the parameters are dependent upon the experiments, the more robust the model is. Thirdly, unlike the conventional numerical methods based on discretizations of macroscopic continuum equations, LB method is based on microscopic models and mesoscopic kinetic equations for fluids, the kinetic nature of which enables it to be applicable for micro-flow.

Therefore, the present electrochemical model shows much more excellent behavior under the vast majority of the SOFC operating conditions because of the much more precise prediction of the concentration overpotential using the LB method, and it also indicates that the accurate simulation of mass transfer in the electrode affects the overall overpotential greatly.

4.2. Parametric analysis

Although several papers have investigated the effects of macroscopic geometrical and operating parameters on the cell electrochemical performance, they are based on the traditional mass transfer models and the accuracy of them calls for further improvement [2,14,35]. Precise simulation of the SOFC electrochemical performance is the premise of the valid parameter study which is the basis for cell design and operation. The validated electrochemical model based on LB method in this paper is applied to gain the understanding of cell performance under different conditions, and it is also a further validation of the newly built model.

4.2.1. Standard case

Since the performance of the anode-supported SOFC is more desirable than that of both cathode- and electrolyte-supported SOFC [13], the subsequent study is focused on an anode-supported SOFC. The input parameters of the standard case are described in Table 2 [35,37].

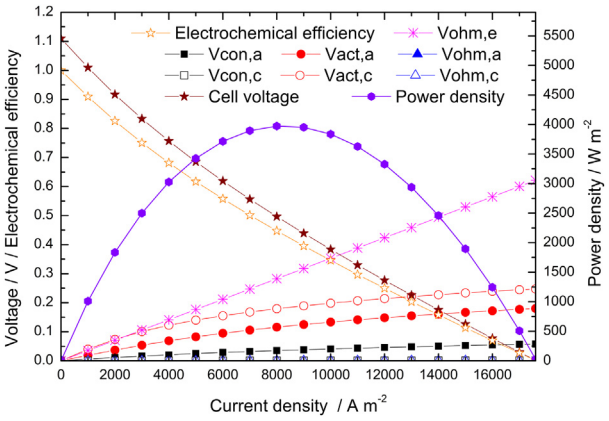

Fig. 4. Performance of anode-supported SOFC of the standard case.

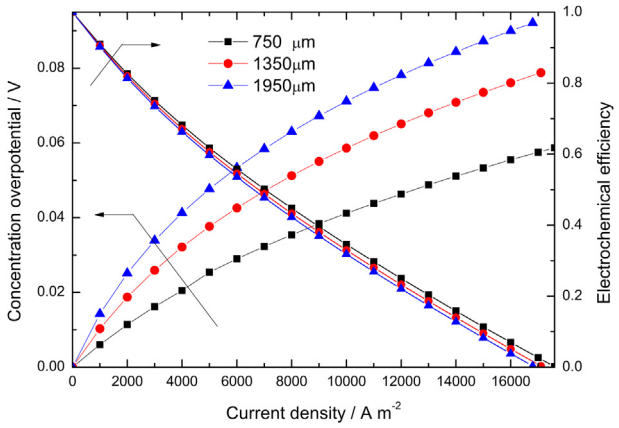

Fig. 5. Effects of anode thickness on concentration overpotential and electrochemical efficiency.

Fig. 4 illustrates the performance of an anode-supported SOFC of the standard case. The cell voltage presents a concave trend due to the protruding tendency of both activation and concentration polarizations. When the current density reaches approximately 8000 A m^{-2}, the cell voltage is 0.5 V, the electrochemical efficiency is 45%, and the power density arrives at its maximum (3974 W m^{-2}). The cell voltage drops to zero when the current density is about 17,600 A m^{-2}. The maximum loss comes from the electrolyte ohmic polarization. This is mainly because of the high ionic resistivity of electrolyte and relatively low operating temperature (1023 K). In contrast, the electronic resistivity of electrodes is so low that the electrode ohmic polarization approximates to zero. Meanwhile, the activation overpotentials of both electrodes are also very high, especially the cathode polarization due to its lower exchange current density. Concentration polarization is relatively smaller, and the contribution of cathode to it is close to zero because of its low thickness. It is also clear in Fig. 4 that with the increase of the current density, anode concentration loss rises gradually due to the fuel starvation at anode–electrolyte interface for the reactant gases fail to diffuse through the electrode quickly in the high current density region. Finally, it will be of the same order of magnitude of other overpotentials, and neglecting it or employing fitted limiting current density and relevant simplified macroscopic models (e.g. extended FM, SMM and DGM) will undoubtedly cause inaccurate results.

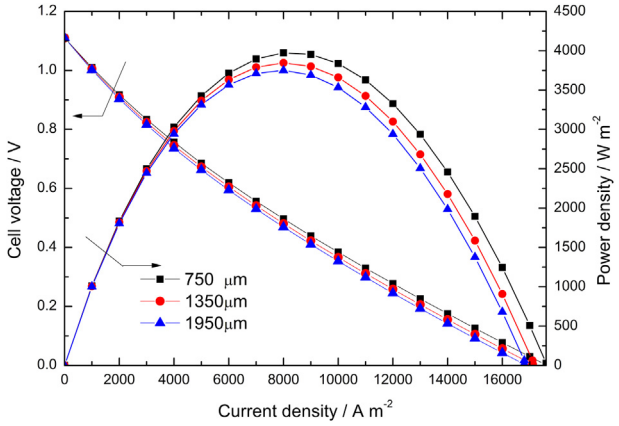

Fig. 6. Effects of anode thickness on cell voltage and power density.

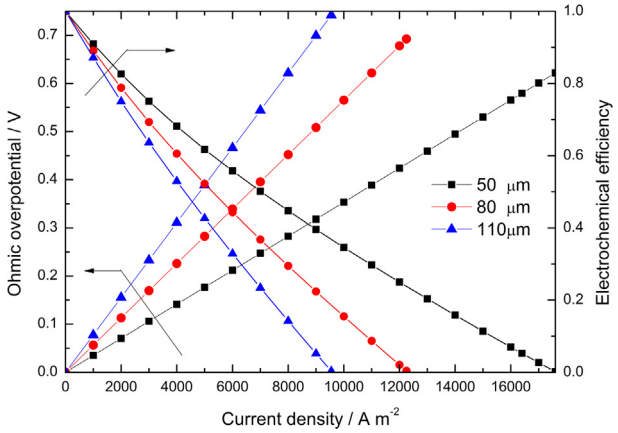

Fig. 7. Effect of electrolyte thickness on ohmic overpotential and electrochemical efficiency.

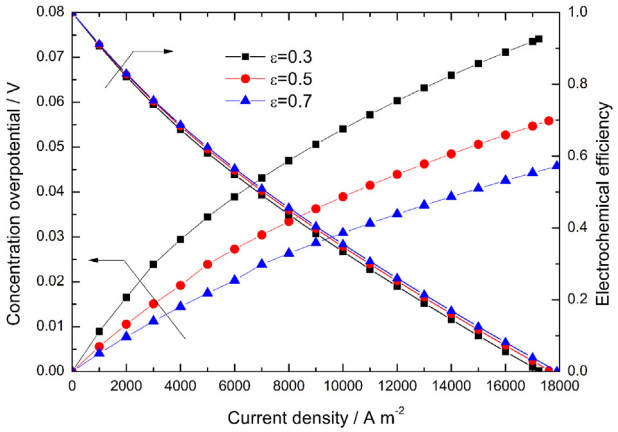

Fig. 9. Effect of porosity on concentration overpotential and electrochemical efficiency.

4.2.2. *Effects of anode thickness*

Figs. 5 and 6 illustrate the impacts of anode thickness on concentration overpotential, electrochemical efficiency, cell voltage and power density. With the rise of the anode thickness, higher resistance to the reactant gas species transported in the porous anode occurs, which brings about the increase of the concentration polarization, as well as the decrease of the cell voltage, electrochemical efficiency, power density and the operating current density range with the subsequent inferior cell performance. Moreover, the sensitivity of concentration overpotential to the anode thickness reduces with the increase of the anode thickness. So an anode-supported SOFC with a relatively thicker anode is acceptable since the concentration polarization will not accrete excessively. However, for the sake of the improvement of the cell performance to the greatest extent, the thinner the anode is, the better, as long as it is thick enough to support the cell.

4.2.3. *Effects of electrolyte thickness*

The influences of electrolyte thickness on ohmic loss, electrochemical efficiency, cell voltage and power density are shown in Figs. 7 and 8. When the electrolyte thickness goes up, the ohmic loss increases; meanwhile, the cell voltage, power density and electrochemical efficiency present inverse tendencies. According to Eq. (8), ohmic polarization varies linearly with the electrolyte thickness. So it is suggested that the electrolyte should be as thin as possible only if it meets the mechanics requirements of the cell structure, and the material with lower ionic resistivity is recommended for the electrolyte so as to reduce the ohmic polarization.

4.2.4. *Effects of porosity*

Figs. 9 and 10 depict the effects of porosity on SOFC performance. With the porosity increasing, the reduced concentration overpotential and improved cell performance appear due to the enhanced gas diffusion in the porous electrodes, and the sensitivity of concentration polarization and cell performance to the increase of porosity decreases gradually, which means that the precise calculation of concentration is relatively more crucial in low porosity regions. However, the increase of the porosity leads to the reduction of the length of TPB where the electrochemical reaction takes place. Hence, in a typical anode-supported SOFC, adjacent to the electrolyte are electrocatalytic layers of anode and cathode with low porosity, which is helpful for the electrochemical reaction. In contact with the electrocatalytic layers is the porous structure with high porosity, which benefits the reactant gas transport.

4.2.5. *Effects of fuel composition*

Ref. [35] adopted the extended FM to calculate the concentration overpotential and indicated that the rise of the molar fraction of hydrogen caused the reduction of the concentration polarization. However, we've obtained different conclusions with LB model as is illustrated in Fig. 11. When the molar fraction of hydrogen ascends, the concentration polarization declines at first, and then goes up. However, the EMF overlaps with each other at different current

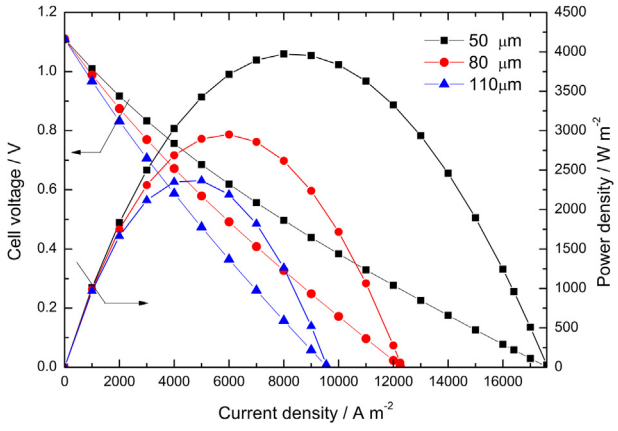

Fig. 8. Effect of electrolyte thickness on cell voltage and power density.

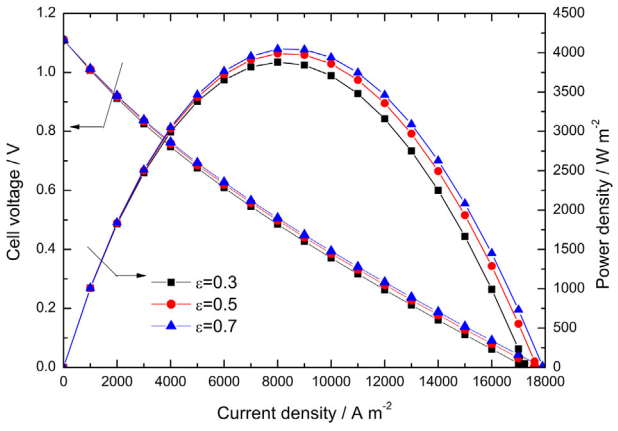

Fig. 10. Effect of porosity on cell voltage and power density.

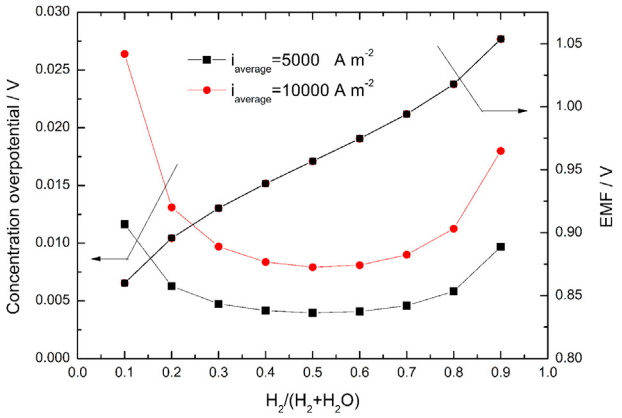

Fig. 11. Effect of hydrogen molar fraction on concentration overpotential and EMF.

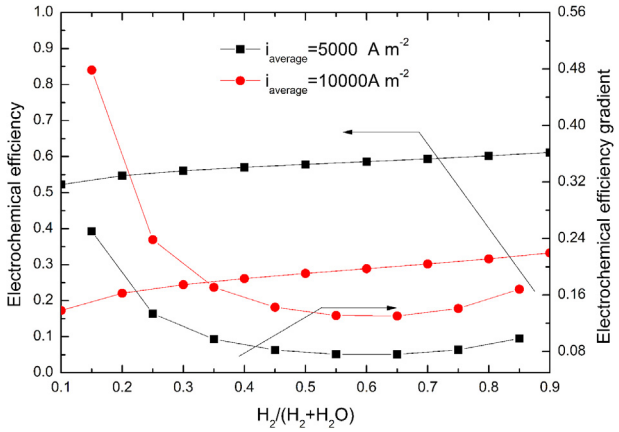

Fig. 13. Effect of hydrogen molar fraction on electrochemical efficiency and its gradient.

densities and increases all the way. As average current density increases, both activation and ohmic polarizations present rising tendencies and keep constant at different hydrogen molar fraction according to Eqs. (7) and (8). So the cell voltage rises as hydrogen molar fraction increases and falls as average current density ascends (see Fig. 12), and it changes even faster than EMF, which brings about the increasing trend of electrochemical efficiency as is shown in Fig. 13. It is also clear in Fig. 13 that the sensitivity of electrochemical efficiency to hydrogen molar fraction initially reduces greatly, then slightly rises in regions of high hydrogen molar fraction, and the value is much smaller when the average current density decreases, which means that the accuracy of concentration polarization prediction is much more crucial for low reactant concentrations and high average current densities.

4.2.6. Effects of operating temperature

Figs. 14 and 15 describe the effects of operating temperature on SOFC performance. In Fig. 14, ohmic overpotential declines dramatically with the increase of the operating temperature because the ionic resistivity of the electrolyte is very sensitive to the temperature and drops rapidly with the rising temperature. Similarly, the activation overpotential presents the same tendency as that of ohmic overpotential because a higher operating temperature leads to more reactive electrodes. Conversely, the concentration polarization shows an increasing tendency when the operating temperature rises. However, the magnitude of the increase of concentration overpotential is relatively small compared with the decrease of ohmic and activation overpotentials. As a result, a better cell performance can be obtained in higher operating temperature regions (see Fig. 15). It is also clear in Figs. 14 and 15 that the operating temperature has the most significant effect on the cell performance compared with other parameters. In general, during the operation process of SOFC, the cell operating temperature is directly affected by the three polarization losses, which indicates the importance of more accurate prediction of concentration polarization once again.

5. Conclusions

An electrochemical model is developed and well validated to investigate the performance of an anode-supported SOFC. Unlike other existing electrochemical models, the present simulation has employed a LB model based on two-fluid theory at REV scale to describe the multi-component gas transport and the concentration polarization in porous electrodes of SOFC. The impacts of geometrical and operating parameters on overpotentials, electrochemical efficiency, cell voltage and power density of a planar type anode-supported SOFC are discussed, which also serves as a further validation of the present electrochemical model.

The volt–ampere characteristics of the SOFC obtained by the present electrochemical model based on the LB algorithm at REV scale almost overlap with the experimental data [36] under the bulk of the SOFC operating conditions (below about 15,000 A m^{-2}), and also agree better with the measured value [36] than the results

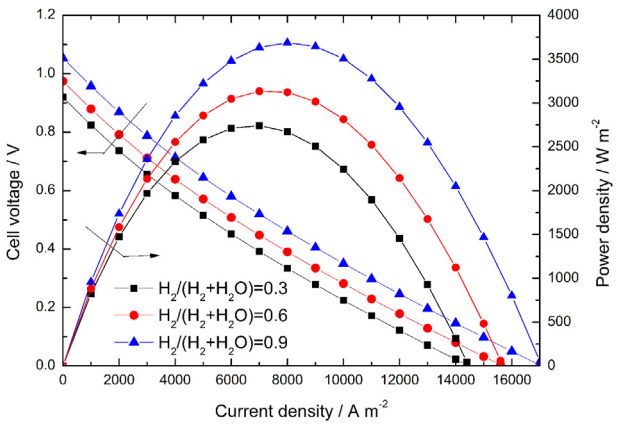

Fig. 12. Effect of hydrogen molar fraction on cell voltage and power density.

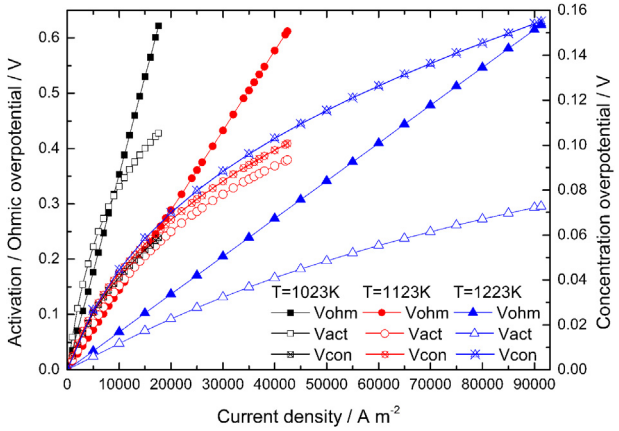

Fig. 14. Effect of operating temperature on overpotentials.

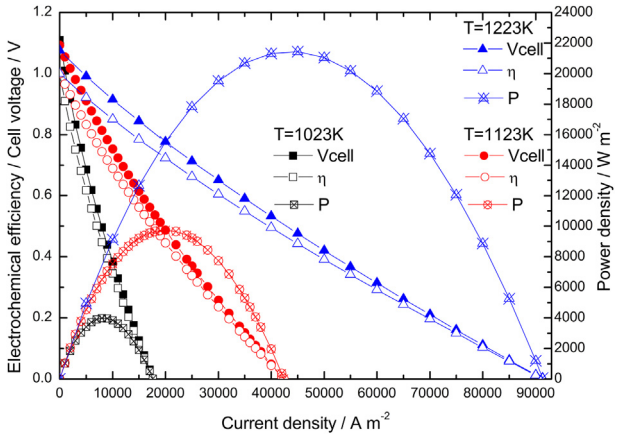

Fig. 15. Effects of operating temperature on cell voltage, electrochemical efficiency and power density.

given by Ni et al. [35] for high current densities (above about 15,000 A m^{-2}), which not only confirms the reliability of the present electrochemical model, but also proves that the precise simulation of mass transfer affects the accurate prediction of the SOFC electrochemical performance greatly.

The anode and electrolyte are suggested to be as thin as possible as long as meet the mechanics requirements for the cell structure, and the electrolyte material of low ionic resistivity is recommended to reduce the ohmic polarization; with the porosity increasing, the decreased concentration overpotential and the better cell performance appear; when the hydrogen molar fraction rises, the concentration polarization of SOFC initially declines, and then goes up, and the electrochemical efficiency represents an overall increasing tendency; enhancing the operating temperature, the activation and ohmic overpotentials fall markedly, the concentration overpotential experiences a slight rise, and thus the cell performance improves.

The accurate prediction of concentration polarization is of great importance for the cell performance simulation, especially for thicker electrode, low porosity, low reactant concentrations and high average current densities.

The developed electrochemical model based on LB algorithm at REV scale is capable of studying the macroscopic performance of SOFC accurately and effectively because of its kinetic nature at microscale or mesoscale, and proves to be beneficial for the design and optimization of SOFC.

Acknowledgments

This work is supported by National Natural Science Foundation of China (50976092), specialized Research Fund for the Doctoral Program of Higher Education of China (20090201120076), and the Fundamental Research Funds for the Central Universities.

Nomenclature

$\vec{e}$	discrete lattice velocity
E	electromotive force, V
f	particle mass distribution function
$f_\alpha^{\sigma(0)}$	equilibrium distribution function in two-fluid model
$f_\alpha^{\sigma(\mathrm{eq})}$	equilibrium distribution function
F	Faraday constant, 96,485 C mol^{-1}
Δg	molar Gibbs free energy change, J mol
i	current density, A m^{-2}
j	current, C s^{-1}
J	mass flux, kg m^{-3} s^{-1}
$J_\alpha^{\sigma\sigma}$	self-collision term
$J_\alpha^{\sigma s}$	cross-collision term
K	permeability, m^2
p	pressure, Pa
P	power density, W m^{-2}
r	resistance, Ω
R	gas constant, J mol^{-1} K^{-1}
T	temperature, K
$\vec{u}$	velocity of fluid, m s^{-1}
$V_{\mathrm{act,a}}$	activation overpotential of anode, V
$V_{\mathrm{act,c}}$	activation overpotential of cathode, V
V_{cell}	output voltage, V
$V_{\mathrm{con,a}}$	concentration overpotential of anode, V
$V_{\mathrm{con,c}}$	concentration overpotential of cathode, V
V_{ohm}	ohmic overpotential, V
$\vec{x}$	position vector
y_i	molar fraction of component i

Greek symbols

α	lattice direction
δt	time step
ε	porosity
η	electrochemical efficiency
μ	viscosity of fluid, kg m^{-1} s^{-1}
ρ	density, kg m^{-3}
τ^σ	relaxation time of self-collision term
$\tau_{\mathrm{D}}^{\sigma s}$	relaxation time of cross-collision term

Subscripts

a	anode
A/E	interface between anode and electrolyte
c	cathode
C/E	interface between cathode and electrolyte
e	electrolyte
eff	effective

Superscripts

σ	species σ
s	species s

References

[1] Wojciech MB, Jaroslaw M. Solid-oxide fuel cells in power generation applications: a review. Recent Pat Eng 2011;5:165–89.
[2] Arpino F, Massarotti N. Numerical simulation of mass and energy transport phenomena in solid oxide fuel cells. Energy 2009;34:2033–41.
[3] Lawlor V, Griesser S, Buchinger G, Olabi AG, Cordiner S, Meissner D. Review of the micro-tubular solid oxide fuel cell: part I. Stack design issues and research activities. J Power Sources 2009;193:387–99.
[4] Hofmann P, Panopoulos KD, Fryda LE, Kakaras E. Comparison between two methane reforming models applied to a quasi-two-dimensional planar solid oxide fuel cell model. Energy 2009;34:2151–7.
[5] Song TW, Sohn JL, Kim JH, Kim TS, Ro ST, Suzuki K. Performance analysis of a tubular solid oxide fuel cell/micro gas turbine hybrid power system based on a quasi-two dimensional model. J Power Sources 2005;142:30–42.
[6] Costamagna P, Magistri L, Massardo AF. Design and part-load performance of a hybrid system based on a solid oxide fuel cell reactor and a micro gas turbine. J Power Sources 2001;96:352–68.
[7] Bang-Møller C, Rokni M, Elmegaard B, Ahrenfeldt J, Henriksen UB. Decentralized combined heat and power production by two-stage biomass gasification and solid oxide fuel cells. Energy 2013;58:527–37.
[8] Chakraborty UK. Static and dynamic modeling of solid oxide fuel cell using genetic programming. Energy 2009;34:740–51.
[9] Rokni M. Thermodynamic analysis of SOFC (solid oxide fuel cell)–Stirling hybrid plants using alternative fuels. Energy 2013;61:87–97.
[10] Liso V, Olesen AC, Nielsen MP, Kær SK. Performance comparison between partial oxidation and methane steam reforming processes for solid oxide fuel cell (SOFC) micro combined heat and power (CHP) system. Energy 2011;36:4216–26.
[11] Doherty W, Kennedy Reynolds A. Computer simulation of a biomass gasification-solid oxide fuel cell power system using Aspen Plus. Energy 2010;35:4545–55.

[12] Calise F, Dentice d'Accadia M, Palombo A, Vanoli L. Simulation and exergy analysis of a hybrid solid oxide fuel cell (SOFC)–gas turbine system. Energy 2006;31:3278–99.
[13] Iwai H, Yamamoto Y, Saito M, Yoshida H. Numerical simulation of intermediate-temperature direct-internal-reforming planar solid oxide fuel cell. Energy 2011;36:2225–34.
[14] Chan SH, Khor KA, Xia ZT. A complete polarization model of a solid oxide fuel cell and its sensitivity to the change of cell component thickness. J Power Sources 2001;93:130–40.
[15] Xu H, Dang Z, Bai BF. Numerical simulation of multispecies mass transfer in a SOFC electrodes layer using lattice Boltzmann method. J Fuel Cell Sci Technol 2012;9:061004.
[16] Joshi AS, Peracchio AA, Grew KN, Chiu WKS. Lattice Boltzmann method for continuum, multi-component mass diffusion in complex 2D geometries. J Phys D: Appl Phys 2007;40:2961–71.
[17] Joshi AS, Peracchio AA, Grew KN, Chiu WKS. Lattice Boltzmann method for multi-component, non-continuum mass diffusion. J Phys D: Appl Phys 2007;40:7593–600.
[18] Joshi AS, Grew KN, Peracchio AA, Chiu WKS. Lattice Boltzmann modeling of 2D gas transport in a solid oxide fuel cell anode. J Power Sources 2007;164:631–8.
[19] Chiu WKS, Joshi AS, Grew KN. Lattice Boltzmann model for multi-component mass transfer in a solid oxide fuel cell anode with heterogeneous internal reformation and electrochemistry. Eur Phys J Spec Top 2009;171:159–65.
[20] Grew KN, Joshi AS, Peracchio AA, Chiu WKS. Pore-scale investigation of mass transport and electrochemistry in a solid oxide fuel cell anode. J Power Sources 2010;195:2331–45.
[21] Joshi AS, Grew KN, Izzo JR, Peracchio AA, Chiu WKS. Lattice Boltzmann modeling of three-dimensional, multicomponent mass diffusion in a solid oxide fuel cell anode. J Fuel Cell Sci Technol 2010;7:0110061–8.
[22] Suzue Y, Shikazono N, Kasagi N. Micro modeling of solid oxide fuel cell anode based on stochastic reconstruction. J Power Sources 2008;184:52–9.
[23] Asinari P, Quaglia MC, von Spakovsky MR, Kasula BV. Numerical simulations of reactive mixture flow in the anode layer of solid oxide fuel cells by the lattice Boltzmann method. In: Proceedings of ESDA 2006, Torino, Italy; 2006.
[24] Martys NS, Chen H. Simulation of multicomponent fluids in complex three-dimensional geometries by the lattice Boltzmann method. Phys Rev E 1996;53:743–50.
[25] Spaid MAA, Phelan FR. Lattice Boltzmann methods for modeling microscale flow in fibrous porous media. Phys Fluids 1997;9:2468–74.
[26] Spaid MAA, Phelan FR. Modeling void formation dynamics in fibrous porous media with the lattice Boltzmann method. Compos A: Appl Sci Manuf 1998;29:749–55.
[27] Park J, Matsubara M, Li X. Application of lattice Boltzmann method to a micro-scale flow simulation in the porous electrode of a PEM fuel cell. J Power Sources 2007;173:404–14.
[28] Lu Q, Huang G. A simulation of gas migration in heterogeneous goaf of fully mechanized coal caving mining face based on multi-components LBM. In: Proceedings of ESIAT 2009, Wuhan, China; 2009.
[29] Delavar MA, Farhadi M, Sedighi K. Numerical simulation of direct methanol fuel cells using lattice Boltzmann method. Int J Hydrogen Energy 2010;35:9306–17.
[30] Chan SH, Low CF, Ding OL. Energy and exergy analysis of simple solid-oxide fuel-cell power systems. J Power Sources 2002;103:188–200.
[31] Luo LS, Girimaji SS. Theory of the lattice Boltzmann method: two-fluid model for binary mixtures. Phys Rev E 2003;67:0363021–03630211.
[32] Sirovich L. Kinetic modeling of gas mixtures. Phys Fluids 1962;5:908–18.
[33] McCracken ME, Abraham J. Lattice Boltzmann methods for binary mixtures with different molecular weights. Phys Rev E 2005;71:0467041–8.
[34] Guo ZL, Zheng CG, Shi BC. Discrete lattice effects on the forcing term in the lattice Boltzmann method. Phys Rev E 2002;65:0463081–6.
[35] Ni M, Leung MKH, Leung DYC. Parametric study of solid oxide fuel cell performance. Energy Convers Manag 2007;48:1525–35.
[36] Zhao F, Virkar AV. Dependence of polarization in anode-supported solid oxide fuel cells on various cell parameters. J Power Sources 2005;141:79–95.
[37] Yakabe H, Hishinuma M, Uratani M, Matsuzaki Y, Yasuda I. Evaluation and modeling of performance of anode-supported solid oxide fuel cell. J Power Sources 2000;86:423–31.